

Uniform Regulation of a Multi-Section Continuum Manipulator

Ian A. Gravagne and Ian D. Walker
Clemson University, Clemson, SC
igravag@clemson.edu, ianw@ces.clemson.edu

Abstract

Continuum manipulators are robotic manipulators built using one continuous, elastic, and highly deformable “backbone” instead of multiple rigid links and joints. In previous work, we illuminated various kinematic and dynamic properties of continuum robots, but the question of controller design remained open. This paper presents a basic result for continuum robots that has long been known for rigid-link robots: that a simple PD-plus-feedforward controller can exponentially regulate the position of a manipulator.

1 Introduction

“Continuum robots”, a phrase referenced from a survey paper by Robinson and Davies [1], refers to a class of robotic manipulators that essentially discard the traditional robot design paradigm that joins stiff, rigid links with rotational or prismatic joints. That this design methodology has been highly successful in the past is certainly not under debate; in fact, here and in previous work we suggest that rigid-link designs will continue to fulfill the majority of automation and manipulation need for the foreseeable future. However, rigid-link design and analysis seems to have reached some practical limits. Among these, it is difficult and often expensive to design compliance into a rigid-link robot at any point except the end-effector. We are beginning to see that compliance is a critical ingredient in the creation of safe, comfortable and interactive human-robot environments [2]. Compliance is also a significant asset for the manipulation or exploration of unknown environments. Additionally, rigid-link robots generally do not have the ability to use their entire structure to manipulate things, called “whole-arm manipulation”, and tend to be complex to build, heavy (in order to impart stiffness) and somewhat bulky.

Some of the aforementioned issues are being addressed by creative mechanical designs, which often accept some flexibility and vibration in the robot links in exchange for lighter weight, less complexity and greater safety margin. The question at hand is, why not abandon the joints altogether, and make the entire mechanism out of one long flexible member? Inspired by trunks, tentacles and snake backbones, continuum robot designs such as the simple prototype seen in figure 1 attempt to answer this ques-

tion. However, with new properties and capabilities, continuum robots emphasize the need for new or expanded results in some areas that long ago matured for rigid-link robots. In fact, the purpose of this paper is to establish a basic but extremely important result in continuum manipulator control, namely, that a PD-plus-feedforward controller can exponentially regulate the position of a continuum robot – a result long understood for rigid-link designs.

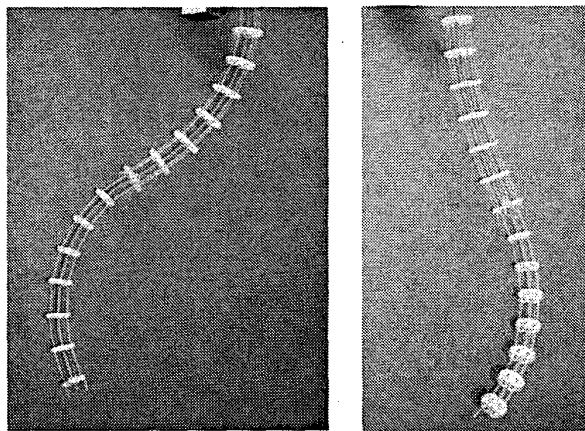


Figure 1: The Clemson Tentacle Manipulator is a two-section, four degree-of-freedom continuum robot.

2 Background

Our work in continuum manipulators grew out of the early studies of hyper-redundant and high-degree-of-freedom (HDOF) devices. Some of the initial HDOF design attempts appear in [3], [4]. More recent designs appear in [5] and [6]. For background into the kinematics and path-planning of continuum and hyper-redundant robots, see [7]- [15]. Also, [10] and [11] discuss the dynamics of continuum planar robots. Some of the fundamentals in this work are derived from the field of elastica mechanics, and details can be found in [17]-[19] and [21].

3 Dynamic Model

The fundamental difference between a rigid-link robot and a continuum robot is that a continuum backbone exhibits infinite-dimensional kinematics, described by differential equations. Because currently practical actuation schemes cannot continuously actuate such a backbone, the range of actuation is limited to a finite-dimensional subspace of the infinite-dimensional kinematics. The “left-over” region permits a desirable property termed “inherent passive compliance”, but also permits the existence of vibrations that, depending on the system configuration and physical properties, may or may not be controllable. (See [11] for an example of uncontrollable axial vibration of a continuum robot.) Uncontrollable modes are only one of several ways that a continuum robot design can tax the theoretical limits of our ability to model and analyze it. For this reason, the majority of our work has so far been limited to planar robots, and in this paper we further restrict the design parameters to non-extensible backbones with distributed damping and negligible shear effects.

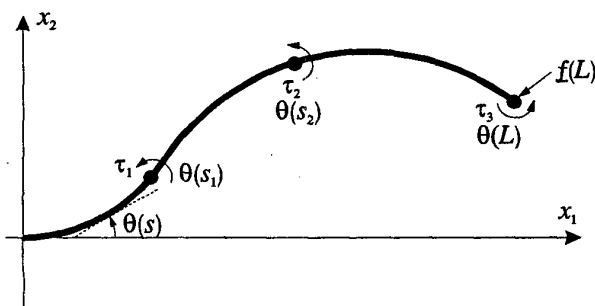


Figure 2: A 3-actuator (3-section) continuum robot. Actuators apply moments to points s_1 , s_2 and $s_3 = L$.

Figure 2 illustrates a backbone of length L . Arc length s ranges from 0 to L , so we employ s as an independent parameter, in addition to time t . Thus, at every point s , the backbone has centerline position $\underline{x}(s, t) = [x_1(s, t) \ x_2(s, t)]^T$, and its tangent subtends angle $\theta(s, t)$ counterclockwise from the horizontal. The backbone has bending stiffness EI , with linear mass density ρ and rotational inertial density I_ρ . The kinetic and potential energies of the robot are then

$$KE = \frac{1}{2} \int_0^L \rho \|\dot{\underline{x}}\|^2 + I_\rho \dot{\theta}^2 ds \quad (1)$$

$$PE = \frac{1}{2} \int_0^L EI (\theta')^2 ds. \quad (2)$$

In addition, deriving the system dynamics requires the

first variation of the work W ,

$$\delta W = \int (-b\dot{\theta})\delta\theta ds + \tau_n\delta\theta(L, t) + \sum_{i=1}^{n-1} \tau_i\delta\theta(s_i, t), \quad (3)$$

$$0 < s_1 < \dots < s_{n-1} < L.$$

The term inside the integral represents energy “extracted” from the system by a linear viscoelastic damping mechanism with damping coefficient b . The remaining terms reflect intermediate actuator input torques τ_1 to τ_{n-1} , applied at points s_1 to s_{n-1} , as well as boundary torque τ_n applied at $s_n = L$. Note that the work does not reflect the presence of external shear/axial inputs, because the robot does not possess actuators capable of applying those types of forces.

To ease the notational and calculational complexities associated with the intermediate actuators, we rewrite the last term above as

$$\sum_{i=1}^{n-1} \tau_i\delta\theta(s_i, t) = \int_0^L \left[\sum_{i=1}^{n-1} \tau_i(t)\delta(s - s_i) \right] \delta\theta(s, t) ds \quad (4)$$

where $\delta(s_i)$ is the Dirac delta distribution, not to be confused with the variational operator. (The notation should be contextually clear.) Then, we define the “distributed moment” as

$$m(s, t) \triangleq \sum_{i=1}^{n-1} \tau_i(t)\delta(s - s_i) \quad (5)$$

so that the new virtual work expression is

$$\delta W = \int (m - b\dot{\theta})\delta\theta ds + \tau_n\delta\theta(L, t). \quad (6)$$

Using the previously defined potential and kinetic energies, the dynamics can be derived as [22], [21]

$$-I_\rho\ddot{\theta} - b\dot{\theta} + \underline{f}^T T^T \underline{q} + EI\theta'' + m = 0 \quad (7a)$$

$$\underline{f}' - \rho\dot{\underline{x}} = \underline{0} \quad (7b)$$

$$EI\theta'(L, t) = \tau_n \quad (7c)$$

$$\underline{f}(L, t) = \underline{0} \quad (7d)$$

along with the geometric conditions $\theta(0, t) = 0$ and $\underline{x}(0, t) = \underline{0}$. In a non-extensible thin beam with relatively large shear modulus, the tangent vector obeys[12]

$$\underline{x}'(s, t) = \begin{bmatrix} \cos(\theta) \\ \sin(\theta) \end{bmatrix} \triangleq \underline{q}(s, t) \quad (8)$$

and it easily follows that

$$\delta\underline{x}' = T^T \underline{q} \delta\theta; \quad T = \begin{bmatrix} 0 & 1 \\ -1 & 0 \end{bmatrix}, \quad (9)$$

a relationship that we will employ repeatedly in the coming derivations. Note that primes indicate partial differentiation $\frac{\partial}{\partial s}$.

The force $f(s, t)$ in (7a) identifies closely with the role of a temporary variable. Because we have chosen to neglect the effects of shear and axial deformations – a physically realistic assumption for thin backbones – f does not relate directly to the primary system position coordinates, and consequently does not have an associated governing equation. (Note that its relation to θ is direct in the case of more complicated models that account for shear, e.g. [21].) Regardless of whether shear/axial forces contribute to the deformation of the backbone, they do exist and boundary condition (7d) reflects the static shear/axial end-effector loading, if there is any. For simplicity here, we assume such loading is negligible but also remark that this is another important difference between continuum robots and traditional robots: end-effector loads *do* deform the robot's shape, and must be accounted for in the kinematics as well as the dynamics. Details of the preceding dynamic derivation appear in [22].

4 Regulation Stability

A regulation controller attempts to drive the system to some desired “set-point”. For an infinite-dimensional device with only a finite number of actuators, the desired system solution $\theta_d(s)$ must be restricted to a class of functions defined by the allowable static system solutions. Specifically, canceling the time-derivative terms in (7) yields

$$EI\theta_d''(s) + \sum_{i=1}^{n-1} \tau_{d,i} \delta(s - s_i) = 0 \quad (10a)$$

$$EI\theta_d'(L) = \tau_{d,n} \quad (10b)$$

where $\tau_{d,i}$ is the i^{th} desired static backbone moment applied by the actuators. These solutions correspond to shapes consisting of semi-circular sections end-to-end, as explored in [11] and [12].

Now consider the control law

$$\tau_i = \tau_{d,i} - k_{d,i} \dot{\theta}(s_i, t) - k_{p,i} \tilde{\theta}(s_i, t) \quad (11)$$

where $\tau_{d,i}$ are the desired static holding torques and $k_{d,i} > 0$. Referring to (7c) and (10b), this gives the boundary control law

$$EI\tilde{\theta}'(L, t) = -k_{d,n} \dot{\theta}(L, t) - k_{p,n} \tilde{\theta}(L, t) \quad (12)$$

where $\tilde{\theta} = \theta - \theta_d$.

The energy-based Lyapunov candidate

$$V_1 = \frac{1}{2} \int_0^L \rho \|\dot{\underline{x}}\|^2 + I_\rho \dot{\theta}^2 + EI (\tilde{\theta}')^2 ds + \sum_{i=1}^n \frac{k_{p,i}}{2} \tilde{\theta}(s_i, t)^2 \quad (13)$$

has time derivative

$$\dot{V}_1 = \int_0^L \rho \dot{\underline{x}}^T \ddot{\underline{x}} + I_\rho \ddot{\theta} + EI \dot{\theta}' \tilde{\theta}' ds + \sum_{i=1}^n k_{p,i} \tilde{\theta}(s_i, t) \dot{\theta}(s_i, t). \quad (14)$$

Substituting for the dynamics gives, after integration by parts and some cancelation,

$$\begin{aligned} \dot{V}_1 &= \int_0^L \dot{\theta} (-b\dot{\theta} + m + EI\theta'') - EI\dot{\theta}\tilde{\theta}'' ds \quad (15) \\ &\quad + EI\dot{\theta}(L, t)\tilde{\theta}'(L, t) + \sum_{i=1}^n k_{p,i} \tilde{\theta}(s_i, t) \dot{\theta}(s_i, t) \\ &= \int_0^L \dot{\theta} \left[-b\dot{\theta} + \sum_{i=1}^{n-1} \tau_{d,i} \delta(s - s_i) + EI\theta_d'' \right] ds \\ &\quad - \sum_{i=1}^{n-1} k_{d,i} \dot{\theta}(s_i, t)^2 - k_{d,n} \dot{\theta}(L, t)^2 \\ &= \int_0^L -b\dot{\theta}^2 ds - \sum_{i=1}^n k_{d,i} \dot{\theta}(s_i, t)^2. \end{aligned}$$

Note that (10a) was used in the second step, a legal substitution because (10a) consists only of desired, time-independent quantities and thus remains valid at all times. Thus, the individual quantities in V remain bounded for any given set of initial conditions and desired backbone moments, and furthermore, since $\theta(s, t)^2 \leq L \int_0^L (\tilde{\theta}')^2 ds$, then $\tilde{\theta}$ is point-wise bounded as well, a fact that will be employed in the next section.

5 Regulation Convergence

The new Lyapunov candidate is

$$V = V_1 + V_2 \quad (16)$$

$$V_2 = \varepsilon \int_0^L I_\rho \dot{\tilde{\theta}} + \rho \left(\int_0^s \tilde{\theta} \underline{q}^T T d\sigma \right) \dot{\underline{x}} + \frac{1}{2} b \tilde{\theta}^2 ds \quad (17)$$

where V_1 is given in the previous section. First we prove that $V > 0$ for a sufficiently small $\varepsilon > 0$. With use of the standard inequalities

$$\int_0^L w(s)^2 ds \leq L^2 \int_0^L w'(s)^2 ds \quad \text{for } w(0) = 0 \quad (18)$$

$$pq \leq \alpha p^2 + \frac{1}{\alpha} q^2 \quad \text{for } \alpha > 0 \quad (19)$$

we may upper bound V_2 as

$$\begin{aligned} V_2 &\leq \varepsilon \int_0^L \left\{ I_\rho \dot{\tilde{\theta}}^2 + I_\rho L^2 (\tilde{\theta}')^2 + \rho L^2 \tilde{\theta}^2 + \rho \dot{\underline{x}}^T \dot{\underline{x}} \right. \\ &\quad \left. + \frac{1}{2} b L^2 (\tilde{\theta}')^2 \right\} ds \\ &\leq \varepsilon \int_0^L I_\rho \dot{\tilde{\theta}}^2 + L^2 \left(I_\rho + \frac{1}{2} b + \rho L^2 \right) (\tilde{\theta}')^2 + \rho \dot{\underline{x}}^T \dot{\underline{x}} ds. \end{aligned} \quad (20)$$

Consequently, we may choose ε sufficiently small that V remains positive definite.

At this point we make the important observation that, while V_1 appears to be positive definite in four generalized coordinates (two linear velocities, one angular velocity

and one curvature), in fact only two are required, $\dot{\theta}(s, t)$ and $\ddot{\theta}(s, t)$. This observation can be formalized by noting that the inequality (18) gives

$$\int_0^L \rho \dot{\underline{x}}^T \dot{\underline{x}} ds \leq L^2 \int_0^L \rho \dot{\theta}^2 ds. \quad (21)$$

So, if we define the “minimal” functional,

$$V^* = \frac{1}{2} \int_0^L \dot{\theta}^2 + (\ddot{\theta}')^2 ds + \sum_{i=1}^n k_{p,i} \bar{\theta}(s_i, t)^2 \quad (22)$$

then we may arrive at new upper and lower bounds for V ,

$$\begin{aligned} C_1 V^* &\leq V \leq C_2 V^* \\ C_1 &= \min \left\{ (1 - \varepsilon)(\rho L^2 + I_\rho), \right. \\ &\quad \left. EI - \varepsilon L^2(2\rho L^2 + 2I_\rho + b), 1 \right\} \\ C_2 &= \max \left\{ (1 + \varepsilon)(\rho L^2 + I_\rho), \right. \\ &\quad \left. EI + \varepsilon L^2(2\rho L^2 + 2I_\rho + b), 1 \right\} \end{aligned} \quad (23)$$

where C_1 and C_2 are constants depending only upon system parameters. Note that C_1 can always be made positive by proper choice of ε .

The time derivative of V is, after some cancelation,

$$\begin{aligned} \dot{V} &= \dot{V}_1 + \varepsilon \int_0^L \left\{ I_\rho \dot{\theta}^2 + \ddot{\theta} (EI\theta'' + m) \right. \\ &\quad \left. + \rho \dot{\underline{x}}^T \dot{\underline{x}} - \rho \left(\int_0^s \ddot{\theta} \ddot{q}^T d\sigma \right) \dot{\underline{x}} \right\} ds. \end{aligned} \quad (24)$$

Integrating the third term in (24) gives (25) [next page]. In second step of (25), by (10a), we are simply subtracting zero but implicitly signifying that we restrict allowable desired solutions $\theta_d(s)$ to those that satisfy (10a). Also note that, in the fourth step, control law (12) was implemented, and in the final step, we choose γ sufficiently small that $(EI - \gamma nL) > 0$. Finally, the last term in (24) gives

$$\begin{aligned} &\int_0^L -\rho \left(\int_0^s \ddot{\theta} \ddot{q}^T d\sigma \right) \dot{\underline{x}} ds \\ &\leq \int_0^L \rho \dot{\underline{x}}^T \dot{\underline{x}} + \rho \left(\int_0^s \ddot{\theta} \ddot{q}^T d\sigma \right) \left(\int_0^s \ddot{q} \ddot{\theta} d\sigma \right) ds \\ &\leq \int_0^L \rho L^2 \dot{\theta}^2 + \rho L^2 \left[\dot{\theta} \ddot{q}^T \right] \left[\ddot{q} \dot{\theta} \right] ds \\ &= \int_0^L \rho L^2 \dot{\theta}^2 + \rho L^2 \left[\dot{\theta}^2 \ddot{\theta}^2 \right] ds \\ &\leq \int_0^L \left[\rho L^2 \left(1 + \max_{s,t} \ddot{\theta}^2 \right) \right] \dot{\theta}^2 ds. \end{aligned} \quad (26)$$

For the last step here, we refer to the section on “Regulation Stability”, where it was proven that, for any initial conditions and finite desired backbone moments, $\dot{\theta}(s, t)^2$

is point-wise bounded. Assembling (21), (25) and (26) together, along with (15), yields

$$\begin{aligned} \dot{V} &\leq \int_0^L - \left\{ b - \varepsilon \rho L^2 \left(2 + \max_{s,t} \ddot{\theta}^2 \right) \right\} \dot{\theta}^2 \\ &\quad - \varepsilon (EI - \gamma nL) (\ddot{\theta}')^2 ds \\ &\quad - \sum_{i=1}^n \left\{ k_{d,i} - \frac{\varepsilon}{\gamma} k_{d,i}^2 \right\} \dot{\theta}(s_i, t)^2 - \sum_{i=1}^n \varepsilon k_{p,i} \bar{\theta}(s_i, t)^2 \end{aligned} \quad (27)$$

Thus, for any given trajectory, ε can always be chosen small enough to ensure that \dot{V} is negative definite. With (23), we have that

$$\begin{aligned} \dot{V} &\leq -\lambda V, \\ \lambda &= \frac{\min \left\{ b - \varepsilon \rho L^2 \left(2 + \max_{s,t} \ddot{\theta}^2 \right), \varepsilon (EI - \gamma nL), \varepsilon \right\}}{C_1} \end{aligned} \quad (28)$$

the solution of which leads to

$$V^*(t) \leq \frac{C_2}{C_1} V^*(0) e^{-\lambda t},$$

exponential convergence of V^* , and consequently point-wise exponential convergence of $\ddot{\theta}(s, t)$. Of course, a given choice of ε for one trajectory may not, in general, be suitable for another trajectory because $\max \ddot{\theta}^2$ may differ between the two.

The reader may note that, in the final analysis, the point dampers associated with each actuator do not contribute to the convergence result. However, we experimentally verified in [11] that additional lumped-parameter damping does in fact significantly improve performance for the PD controller without the feedforward term; thus it is necessary to prove that the point dampers do not disturb the stability and convergence results regardless of their utility in the said results per se.

We make one final remark regarding the presence of rotational inertia, I_ρ . Since linear mass density ρ overwhelmingly eclipses I_ρ for most “long and thin” elastic members, it may be stricken from the preceding derivations (i.e. $I_\rho = 0$). With only slight modification, the essential results remain.

6 Simulation and Conclusions

In [22] we derive a finite-element model for the dynamics of a 2-section continuum robot. Figure 3 illustrates the time plot for the simulated robot with parameters $EI = 1$, $\rho = 0.7$, and $I_\rho = 0.001$. These constants are scaled to realistic ratios for long thin backbones; note how small the rotational density is compared to the inertial density. The robot has unit length, and is driven with control gains of $k_{d,i} = 0.4$ and $k_{p,i} = 20$. The damping coefficient is $b = 3.5$. Figure 4 illustrates a time-lapse image of the robot.

$$\begin{aligned}
\int_0^L \tilde{\theta} (EI\tilde{\theta}'' + m) ds &= \int_0^L \tilde{\theta} \left(EI\tilde{\theta}'' + \sum_{i=1}^{n-1} [\tau_{d,i} - k_{d,i}\dot{\tilde{\theta}}(s_i,t) - k_{p,i}\tilde{\theta}(s_i,t)] \delta(s-s_i) \right) ds \quad (25) \\
&= \int_0^L \tilde{\theta} \left(EI\tilde{\theta}'' - \left\{ EI\tilde{\theta}_d''(s) + \sum_{i=1}^{n-1} \tau_{d,i}\delta(s-s_i) \right\} \right. \\
&\quad \left. + \sum_{i=1}^{n-1} [\tau_{d,i} - k_{d,i}\dot{\tilde{\theta}}(s_i,t) - k_{p,i}\tilde{\theta}(s_i,t)] \delta(s-s_i) \right) ds \\
&= \int_0^L EI\tilde{\theta}\tilde{\theta}'' ds + \sum_{i=1}^{n-1} \tilde{\theta}(s_i,t) [-k_{d,i}\dot{\tilde{\theta}}(s_i,t) - k_{p,i}\tilde{\theta}(s_i,t)] \\
&= \int_0^L -EI(\tilde{\theta}')^2 ds + \sum_{i=1}^{n-1} [-k_{d,i}\dot{\tilde{\theta}}(s_i,t)\tilde{\theta}(s_i,t) - k_{p,i}\tilde{\theta}(s_i,t)^2] + \tilde{\theta}(L,t)EI\tilde{\theta}'(L,t) \\
&= \int_0^L -EI(\tilde{\theta}')^2 ds + \sum_{i=1}^n [-k_{d,i}\dot{\tilde{\theta}}(s_i,t)\tilde{\theta}(s_i,t) - k_{p,i}\tilde{\theta}(s_i,t)^2]; \quad s_n = L \\
&\leq \int_0^L -EI(\tilde{\theta}')^2 ds + \sum_{i=1}^n \left[\frac{1}{\gamma} k_{d,i}^2 \dot{\tilde{\theta}}(s_i,t)^2 + \gamma \tilde{\theta}(s_i,t)^2 - k_{p,i}\tilde{\theta}(s_i,t)^2 \right]; \quad \gamma > 0 \\
&\leq \int_0^L -(EI - \gamma nL)(\tilde{\theta}')^2 ds + \sum_{i=1}^n \left[\frac{1}{\gamma} k_{d,i}^2 \dot{\tilde{\theta}}(s_i,t)^2 - k_{p,i}\tilde{\theta}(s_i,t)^2 \right].
\end{aligned}$$

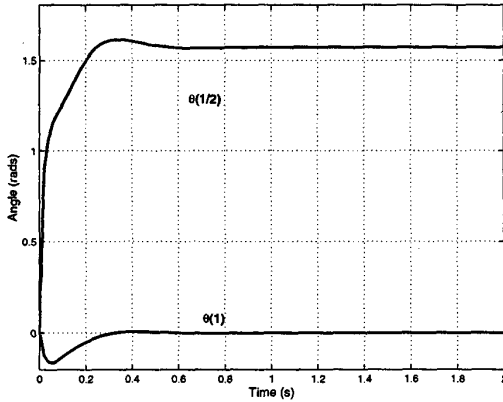


Figure 3: Angles $\theta(\frac{1}{2})$ and $\theta(1)$ for the simulated two-section robot.

To summarize, this work illustrates that a basic control property of rigid-link robots also holds for continuum robots: a PD plus feed-forward controller can exponentially stabilize the system, under the assumption that distributed damping exists on the continuum backbone. Though space does not permit closer examination here, future work will disclose the details leading up to the Lyapunov candidate (16), as well as arguments defending the use of viscous damping on the distributed coordinate $\theta(s,t)$. Reference [12] contains these details, and additional derivations that closely link the structure

of continuum and “traditional” manipulators, lending further credence to the concept of a “unified” theory of manipulation that describes continuum and rigid-link robots simply as special cases.

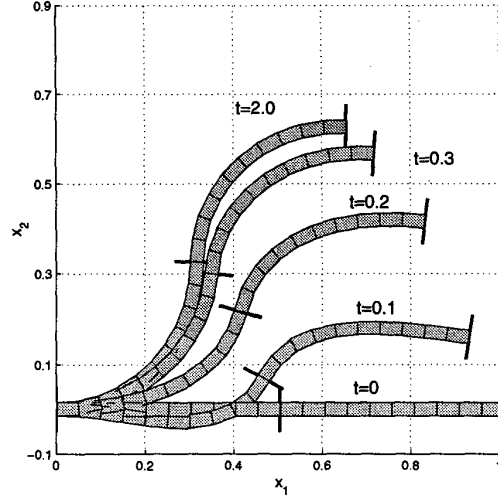


Figure 4: The two-section continuum robot moves from the horizontal straight configuration to the pose $\theta(\frac{1}{2}) = \pi/2$ and $\theta(1) = 0$.

As the idea of continuum robots is still relatively new, a multitude of questions remain unanswered. Among those

that relate to the topic of control, the results above need implementation, and possibly modification to account for types of material damping that do not adopt the standard “viscous” form. In a broader context, the theoretical manipulation capabilities of continuum robots remain obscured by the mathematical complexity of the kinematics, especially in three dimensions.

References

- [1] G. Robinson and J.B.C. Davies, “Continuum Robots – A State of the Art,” Proc. IEEE Int. Conf. Robotics and Automation, Detroit, MI, May 1999, pp. 2849-2854
- [2] H. Lim, K. Tanie, “Human Safety Mechanisms of Human-Friendly Robots: Passive Viscoelastic Trunk and Passively Movable Base,” Int’l Journal of Robotics Research, vol. 19, No. 4, April 2000, pp. 307-335
- [3] S. Hirose, *Biologically Inspired Robots*. Oxford University Press, 1993
- [4] V.C. Anderson and R.C. Horn, “Tensor Arm Manipulator Design,” American Society of Mechanical Engineers, paper #67-DE-57, 1967
- [5] R. Cieslak and A. Morecki, “Elephant Trunk Type Elastic Manipulator - a Tool for Bulk and Liquid Materials Transportation,” *Robotica*, 1999, vol. 17 pp. 11-16
- [6] H. Tsukagoshi, A. Kitagawa, M. Segawa, “Active Hose: An Artificial Elephant’s Nose with Maneuverability for Rescue Operation,” IEEE Int’s Conf. on Robotics and Automation (ICRA), Seoul, Korea, May 2001, pp. 2454-2459
- [7] I.D. Walker and M.W. Hannan, “A Novel Elephant’s Trunk Robot”, IEEE/ASME Intl. Conf. on Advanced Intelligent Mechatronics, Atlanta, GA, Sept. 1999, pp. 410-415
- [8] I. Gravagne and I.D. Walker, “Kinematic Transformations for Remotely-Actuated Planar Continuum Robots,” IEEE Int’l Conf. on Robotics and Automation (ICRA), San Francisco, May 2000, pp. 19-26
- [9] I. Gravagne and I.D. Walker, “On the Kinematics of Remotely-Actuated Continuum Robots,” IEEE Int’l. Conf. on Robotics and Automation (ICRA), San Francisco, May 2000, pp. 2544-2550
- [10] I. Gravagne, C.D. Rahn and I.D. Walker, “Good Vibrations: A Vibration Damping Setpoint Controller for Continuum Robots,” IEEE Int’l Conf. on Robotics and Automation (ICRA), Seoul, Korea, May 2001, pp. 3877-3884
- [11] I. Gravagne, C.D. Rahn and I.D. Walker, “Large Deflection Dynamics and Control for Planar Continuum Robots,” submitted to ASME/IEEE Transaction on Mechatronics
- [12] I. Gravagne and I.D. Walker, “Manipulability and Force Ellipsoids for Continuum Robot Manipulators,” to appear, IEEE/RSJ Int’l Conference on Intelligent Robots and Systems (IROS), Hawaii, October 2001
- [13] M. Hannan and I.D. Walker, “Novel Kinematics for Continuum Robots,” 7th Int’l Symposium on Advances in Robot Kinematics, Piran, Slovenia, June 2000, pp. 227-238
- [14] M. Hannan and I.D. Walker, “Analysis and Initial Experiments for a Novel Elephant’s Trunk Robot,” Int’l Conf. on Intelligent Robots and System (IROS), Takamatsu, Japan, November 2000, pp. 330-337
- [15] G.S. Chirikjian, “Theory and Applications of Hyper-Redundant Robotic Manipulators,” Ph.D. thesis, Dept. of Applied Mechanics, California Institute of Technology, June, 1992
- [16] J.C. Simo, L. Vu-Quoc, “On the Dynamics of Flexible Beams under Large Overall Motions – The Plane Case,” *Journal of Applied Mechanics*, vol. 53, pp.849-863, December 1986
- [17] C.D. Rahn, *Mechatronic Control of Distributed Vibration and Noise*, Expected Publication Aug. 2001.
- [18] J.G. Easley, *Mechanics of Elastic Structures*, Prentice Hall, Englewood Cliffs, NJ, 1989.
- [19] E.H. Love, *A Treatise on the Mathematical Theory of Elasticity*, Dover Publications, NY, 1944
- [20] K. Ito, “Uniform Stabilization of the Dynamic Elastica by Boundary Feedback,” *SIAM J. Control Optim.*, vol. 37, no. 1, pp 316-329, 1998
- [21] J.C. Simo, L. Vu-Quoc, “On the Dynamics of Flexible Beams under Large Overall Motions – The Plane Case,” *Journal of Applied Mechanics*, vol. 53, pp.849-863, December 1986
- [22] I. Gravagne, “On Continuum Robot Control,” Ph.D. Comprehensive Examination Internal Report, ECE Dept., Clemson University